An a posteriori error estimator for the Navier-Stokes equations

Jean-François Hétu* — **André Fortin**** — **Dominique H. Pelletier*****

** Institut des matériaux industriels*
Conseil national de recherche du Canada
75 bld. Montarville, Boucherville
Québec, Canada

*** Département de Mathématiques appliquées*
Ecole Polytechnique de Montréal
Québec, Canada, H3C 3A7

****Département de génie mécanique*
Ecole Polytechnique de Montréal
Québec, Canada, H3C 3A7

RÉSUMÉ. *Nous présentons dans cet article un nouvel estimateur a posteriori de l'erreur pour les équations de Navier-Stockes en régime incompressible. Le principe en est simple : il suffit de calculer deux solutions différentes avec, respectivement, un élément conforme et un élément non conforme. L'estimateur d'erreur est tout simplement la différence entre les deux solutions. Une stratégie de remaillage adaptatif permet ensuite une résolution précise des équations de Navier-Stokes pour les écoulements stationnaires de fluides incompressibles.*

ABSTRACT. *This paper presents an a posteriori error for the incompressible Navier-Stokes equations. Two different solutions are computed, one using the Crouzeix-Raviart element and the second one with the non-conforming Fortin-Soulié element. The error estimator is computed as the difference between these solutions. This estimate is used in an adaptative remeshing strategy for steady state solution of the Navier-Stokes equations.*

MOTS-CLÉS : *estimation d'erreur, fluides incompressibles, éléments conformes et non conformes.*

KEY WORDS : *error estimate, incompressible fluid, conforming and non-conforming elements.*

Revue européenne des éléments finis. Volume 3 – n° 3/1994, pages 363 à 377

1 Introduction

Over the past few years, adaptive methods have stirred much interest because they offer the means of tackling complex flow problems at a reasonable cost. Adaptive methods also provide a framework for controlling the quality and reliability of numerical simulations.

This paper presents such a method for incompressible viscous flows. The solution is first computed with the triangular conforming Crouzeix-Raviart element [CRO 73]. A second solution is then obtained with a non-conforming variant of the Crouzeix-Raviart triangle introduced in Fortin-Soulié [FOR 83]. The local error is linked to the difference between the two solutions. No formal theory exists to support this error estimator.

In order to validate and verify the concept, the estimator is first applied to a problem with a known analytical solution to compare the error estimation with the true error. The method is then applied to the flow over a backward facing step. Predictions are compared with experiments.

So far, no complete theory exists to support the proposed estimator. However, numerical evidence suggests that it is reliable and that it converges towards zero as the adaptive process refines the mesh.

2 The Navier-Stokes Equations

The classical form of the Navier-Stokes equations for an incompressible fluid can be written as:

$$\begin{array}{lcll} \rho(\boldsymbol{u}\cdot\nabla)\boldsymbol{u} & = & -\nabla p+\boldsymbol{f}+\nabla\cdot(\boldsymbol{\sigma}(\boldsymbol{u})) & \text{on } \Omega \\ \nabla\cdot\boldsymbol{u} & = & 0 & \text{on } \Omega \\ \boldsymbol{u} & = & 0 & \text{on } \partial\Omega \end{array} \tag{1}$$

with:

$$\boldsymbol{\sigma}(\boldsymbol{u}) = 2\mu\dot{\boldsymbol{\gamma}}(\boldsymbol{u}) = \mu(\nabla\boldsymbol{u}+(\nabla\boldsymbol{u})^T)$$

where Ω is a bounded, connected polygonal domain in $\mathbb{R}^n$.

In order to solve this problem with the finite element method, we introduce the following Sobolev space and its associated energy norm:

$$V = (H_0^1(\Omega))^n$$

$$\|v\|_{E,\Omega}^2 = \sum_{K\in\mathcal{T}} \|v\|_{E,K}^2 = \sum_{K\in\mathcal{T}} \int_K \boldsymbol{\sigma}(v) : \dot{\boldsymbol{\gamma}}(v)dx \tag{2}$$

We also define a norm on $W = V \times L^2(\Omega)$

$$\|(u,p)\|_{W,\Omega}^2 = \sum_{K\in\mathcal{T}} \|(u,p)\|_{W,K}^2 = \sum_{K\in\mathcal{T}} \left\{ \|u\|_{E,K}^2 + \frac{1}{\mu}\|p\|_{0,K}^2 \right\} \tag{3}$$

where $\mathcal{T}$ is a triangulation of the domain Ω. The continuous variational problem can then be formulated as:

Find $(\boldsymbol{u}, p) \in W$, such that for all $(\boldsymbol{v}, q) \in W$, we have:

$$\begin{aligned} &\int_\Omega \{2\mu\dot{\gamma}(\boldsymbol{u}) : \dot{\gamma}(\boldsymbol{v}) + \rho(\boldsymbol{u} \cdot \nabla \boldsymbol{u}) \cdot \boldsymbol{v} - p\nabla \cdot v\} d\boldsymbol{x} = \int \boldsymbol{f} \cdot v d\boldsymbol{x}, \\ &\int_\Omega q\nabla \cdot \boldsymbol{u} \quad d\boldsymbol{x} = 0 \end{aligned} \tag{4}$$

Problem (4) is then solved by a finite element method.

3 The discrete problem

Problem (4) is solved with two different finite elements shown on figure 1. In both cases the pressure is approximated with piecewise discontinuous linear polynomials. The only difference lies in the bubble function associated to the element controid. For the Crouzeix-Raviart triangle, the bubble is given by:

$$B_{cr} = 27 L_1 L_2 L_3$$

where the L_i are the barycentric coordinates on the triangle. This element ensures continuity of the velocity field across element faces. For the non-conforming Fortin-Soulié element, the bubble is given by:

$$B_{fs} = 2 - 3(L_1^2 + L_2^2 + L_3^2)$$

Because this bubble vanishes only at the gaussian points on the element faces, the velocity across element faces is only continuous at these gaussian points.

Both elements are second order accurate for velocity and pressure. An augmented Lagrangian formulation [FOR 82] is used to solve the discrete problems.

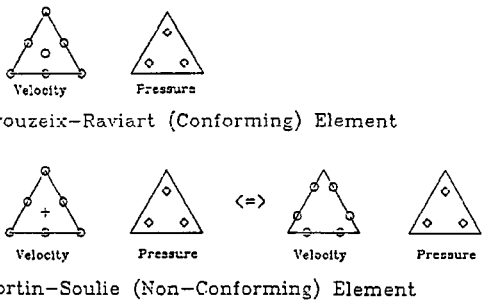

Figure 1. *Conforming and non-conforming elements*

4 A Posteriori Error Estimation

Let $(\boldsymbol{u}^c, p^c)$, $(\boldsymbol{u}^{nc}, p^{nc})$ and $(\boldsymbol{u}, p)$ denote the conforming, non-conforming and analytical velocity-pressure solutions respectively. The objective is to obtain an estimate of the error on each element given two different approximations of the same order. The conforming finite element solution is the one to be analysed for accuracy. Hence the non-conforming one is used as an accessory tool for error estimation.

On each element K, the velocity error is then defined as

$$e_K = ||\boldsymbol{u} - \boldsymbol{u}^c||_{E,K}, \tag{5}$$

that is the energy norm of the difference between the analytical solution and its conforming approximation. Our *a posteriori* error estimation is then defined as

$$e_K^* = ||\boldsymbol{u}^c - \boldsymbol{u}^{nc}||_{E,K}, \tag{6}$$

which is the norm of the difference between the conforming and the non-conforming approximations. We now give a heuristic proof that (6) is an estimator to (5). More precisely, we will show that there exists constants D_1 and D_2 such that

$$D_1 e_K \leq e_K^* \leq D_2 e_K \tag{7}$$

This ensures that a reduction of the error estimate garantees a reduction of the true error. A similar result holds for the pressure.

Since both our elements are second order accurate, their respective errors satisfy

$$\begin{aligned} ||\boldsymbol{u} - \boldsymbol{u}^c||_{E,K} &\simeq C_1 h^2 = e_K, \\ ||\boldsymbol{u} - \boldsymbol{u}^{nc}||_{E,K} &\simeq C_2 h^2 = \frac{C_2}{C_1} e_K \end{aligned} \tag{8}$$

for some constants C_1 and C_2. The following proof is heuristic since the approximation (8) will be taken as an equality. We however believe that the conclusion is valid but this is still to be proven in a more formal manner. The proof requires two steps.

1. The first step uses the Cauchy inequality to find an upper bound for e_K^* and proceeds as follows.

$$\begin{aligned} e_K^* &= ||\boldsymbol{u}^c - \boldsymbol{u}^{nc}||_{E,K} = ||\boldsymbol{u}^c - \boldsymbol{u} + \boldsymbol{u} - \boldsymbol{u}^{nc}||_{E,K} \\ &\leq ||\boldsymbol{u}^c - \boldsymbol{u}||_{E,K} + ||\boldsymbol{u} - \boldsymbol{u}^{nc}||_{E,K} \\ &= (1 + \frac{C_2}{C_1}) e_K = D_2 e_K \end{aligned}$$

2. Two possibilities now exist, depending on wether $C_1 < C_2$ or $C_1 > C_2$. We first have

$$\begin{aligned} e_K &= ||\boldsymbol{u}^c - \boldsymbol{u}||_{E,K} = ||\boldsymbol{u} - \boldsymbol{u}^{nc} + \boldsymbol{u}^{nc} - \boldsymbol{u}^c||_{E,K} \\ &\leq ||\boldsymbol{u} - \boldsymbol{u}^{nc}||_{E,K} + ||\boldsymbol{u}^{nc} - \boldsymbol{u}^c||_{E,K} \\ &\leq \frac{C_2}{C_1} e_k + e_K^* \end{aligned}$$

which leads to

$$(1 - \frac{C_2}{C_1}) e_k \leq e_K^*$$

Unfortunately, if $C_2 > C_1$, $(1 - \frac{C_2}{C_1}) < 0$ and this result is trivial and useless. However, we also have

$$\begin{aligned} (\frac{C_2}{C_1}) e_K &= ||\boldsymbol{u} - \boldsymbol{u}^{nc}||_{E,K} = ||\boldsymbol{u} - \boldsymbol{u}^c + \boldsymbol{u}^c - \boldsymbol{u}^{nc}||_{E,K} \\ &\leq ||\boldsymbol{u} - \boldsymbol{u}^c||_{E,K} + ||\boldsymbol{u}^c - \boldsymbol{u}^{nc}||_{E,K} \\ &\leq e_K + e_K^* \end{aligned}$$

which implies that

$$(\frac{C_2}{C_1} - 1) e_K \leq e_K^*.$$

Since $C_2 > C_1, \frac{C_2}{C_1} - 1 > 0$. Thus for all possible cases we obtain a bound for the error estimator by the error and vice versa. This ensures that a reduction of the error estimator garantees an improvement in the solution.

At first glance, the cost of error estimation may appear prohibitively expensive since two solutions must be computed. Error estimates are in fact obtained at a reasonable cost. First note that the velocity approximation is written in a hierarchical manner:

$$\boldsymbol{u}_h(x, y) = \sum_{i=1}^{6} \boldsymbol{u}_i N_i + \boldsymbol{u}_7 B$$

where the N_i are the standard quadratic shape function and B is the bubble function. Hence, the element degrees of freedom are identical for both element except for the bubble function. This has two consequences:

1. The global stiffness matrices for both approximations are identical except for the terms involving the bubble function (i.e. about 1/3 of the coefficients are different). In other words, the global matrix for the

non-conforming element is a perturbation of that of the conforming triangle.

2. The solution obtained with the conforming element is a very good estimate of the non-conforming solution.

In practice, starting from the conforming solution, one or two iterations are sufficient to obtain the non-conforming solution (to 10^{-3} relative error). In most cases, this represents an increase of 20% to 30% in computations. A cost that is indeed acceptable.

Further saving can be achieved if one iterates for the non-conforming solution using the Newton matrix for the conforming element. In this case, only the residual for the non-conforming element approximation needs to be assembled and no factorization is required.

5 Adaptive strategy

The next key issue lies in how to adapt the mesh given the error estimate. First, we define the velocity and pressure errors as

$$e = u - u^c, \quad \epsilon = p - p^c,$$

and the corresponding estimators

$$e_h = u^c - u^{nc}, \quad \epsilon_h = p^c - p^{nc}.$$

The chosen adaptive strategy is based on remeshing [4,6] and proceeds as follows:

1. Generate an initial mesh
2. Compute a conforming solution
3. Compute a non-conforming solution
4. Compute the error estimate
5. If ($||(e_h, \epsilon_h||_{W,\Omega} >$ Tolerance) then
   (a) Compute grid function (element size) for the improved mesh
   (b) Generate a mesh using the new grid function
   (c) Go to 2
6. else
   (a) Stop, required accuracy has been achieved

The element sizes for the next grid can be evaluated with [4]:

$$\delta_K = \left[\frac{\tau ||(\boldsymbol{u}_h, p_h)||_{W,\Omega}}{\sqrt{N} ||(e_h, \epsilon_h)||_{W,K}} \right]^{1/2} h_K$$

where:

δ_K : the predicted element size for element K
τ : the specified error reduction rate (usually 0.25 or 0.33)
N : the number of elements in the triangulation
h_K : the diameter of element K

This distribution of element size δ_k tends to distribute the error equally on all the elements of the new triangulation $\mathcal{T}$ [ODE 86]. The new mesh is generated by an advancing front technique.[PER 87]

6 Validation

We now present adaptive computations performed on a problem with a known analytical solution which presents a boundary layer. Since the exact solution is readily available, the estimator can be compared to the true error to assess its performance. The solution to this problem is given by:

$$\begin{aligned} \boldsymbol{u} &= (1 - e^{-\alpha y}, 0) \\ p &= 1 - x \\ \alpha &= y\sqrt{\frac{Re}{x}} \\ \Omega &= [0.1; 1.0] \times [0.0; 1.0] \end{aligned}$$

where: $\boldsymbol{u}$ is the the velocity field, α a similarity variable, p the pressure field, Re the Reynolds number and Ω the computational domain. This problem produces a velocity field that closely resembles that of a boundary layer over a flat plate which thickens in the streamwise direction. The transverse velocity component is obtained by integrating the continuity equation from the wall to the free stream. The solution (u, v, p) is substituted into the Navier-Stokes equations (1) and body forces f_x and f_y are computed to ensure that the momentum equations are satisfied.

Figure (2) shows the streamlines for $Re = 200$. It clearly shows the thickening of the boundary layer. This test case retains many non linear terms of (1) thus providing a stringent test for the error estimator. The adaptive strategy attempts to generate improved meshes such that the error is reduced by a factor of three at each adaptive cycle.

The next table summarizes the convergence history of the adaptive process. First one will notice that, as expected, the number of unknowns in-

creases at each adaptive cycle. Rows 2 and 3 indicate that both the error (e, ϵ) and the estimator (e_h, ϵ_h) decrease with each adaptive cycle. This indicating that the estimator is driving the adaptive strategy so as to produce improved solutions at each cycle. The relative errors in row 5 confirms this.

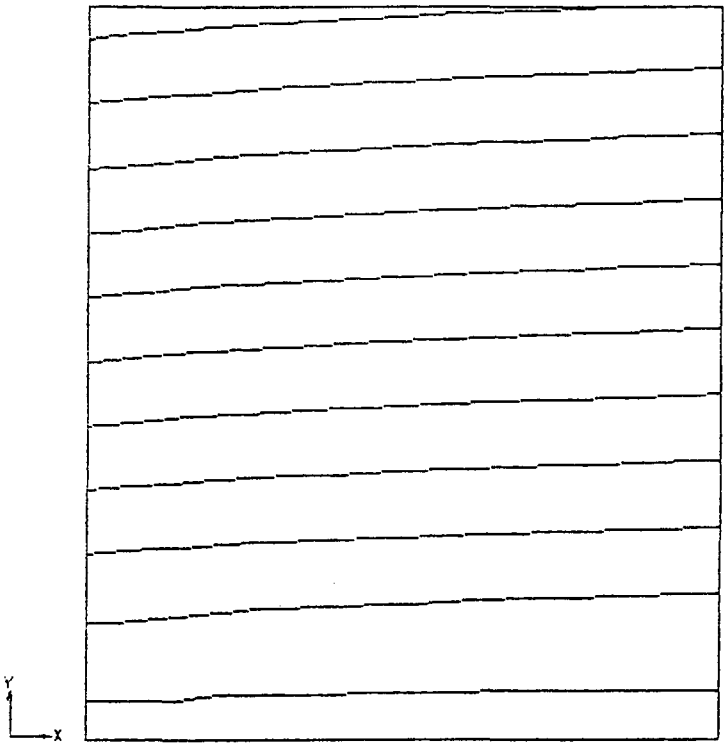

Figure 2. *2-D Boundary Layer : Streamlines*

The fourth row of this table shows that the efficiency θ of the estimator, (which is the ratio of the estimator to the true error) does not tend towards unity. However, the estimator leads to "near" optimal meshes.

Figure (3) shows the initial coarse mesh and the one obtained after 3 cycles of adaptation. Figures (4,5) and (6) clearly shows the convergence of the approximate solution toward the exact one.

Iteration	i	0	1	2	3
Nb Unknowns	neq	283	517	981	2129
True error	$\|\|(e,\epsilon)\|\|_{W,\Omega}$	0.191	0.127	0.032	0.023
Estimator	$\|\|(e_h,\epsilon_h)\|\|_{W,\Omega}$	0.073	0.063	0.019	0.006
Efficiency	$\frac{\|\|(e,\epsilon)\|\|_{W,\Omega}}{\|\|(e_h,\epsilon_h)\|\|_{W,\Omega}}$	0.38	0.49	0.57	0.26
Relative error	$\frac{\|\|(e,\epsilon)\|\|_{W,\Omega}}{\|\|(u,p)\|\|_{W,\Omega}}$	2.7%	1.8%	0.46%	0.32%

7 Application

In this section, we illustrate the usefulness of the proposed error estimator by solving the laminar flow over a backward facing step at $Re = 389$. The geometry and boundary condition are shown in figure 6. Figure 7 shows the initial grid. A parabolic velocity profile is specified at the inlet. No slip is enforced at the walls anf the fluid flows from left to right. The velocity and pressure fields computed on the initial grid are also shown on fig. 8.

Figure 9 shows the results obtained after 2 cycles of adaptation. One can see that the adaptive strategy leads to an improved allocation of elements and nodes. Finally figures 10 and 11 show comparison between predictions and experiments [ARM83] for $Re = 389$. The agreement is excellent everywhere, even at $x/s = 7.76$, a station located immediately downstream of the reattachment point. Good predictions in this region of the flow are notoriously difficult to obtain.

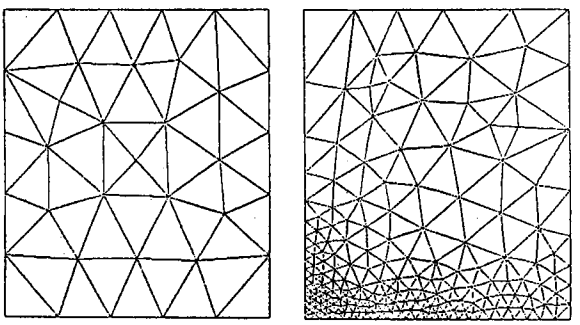

Figure 3. *2-D Boundary Layer : Adaptative Meshes*

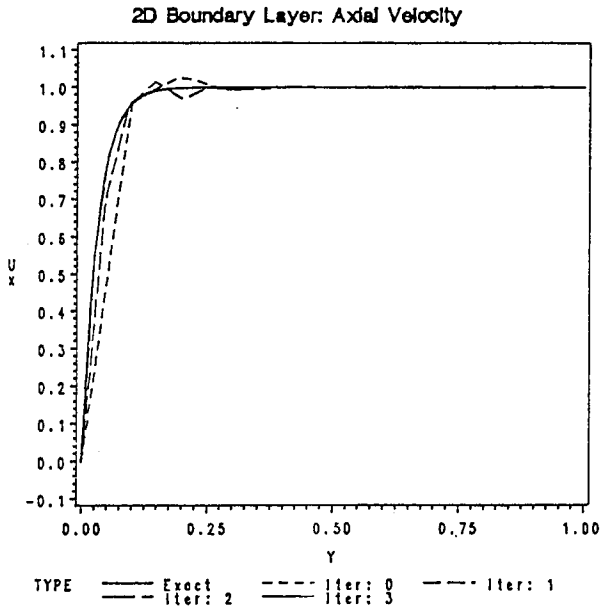

Figure 4. *2-D Boundary Layer : Convergence of u*

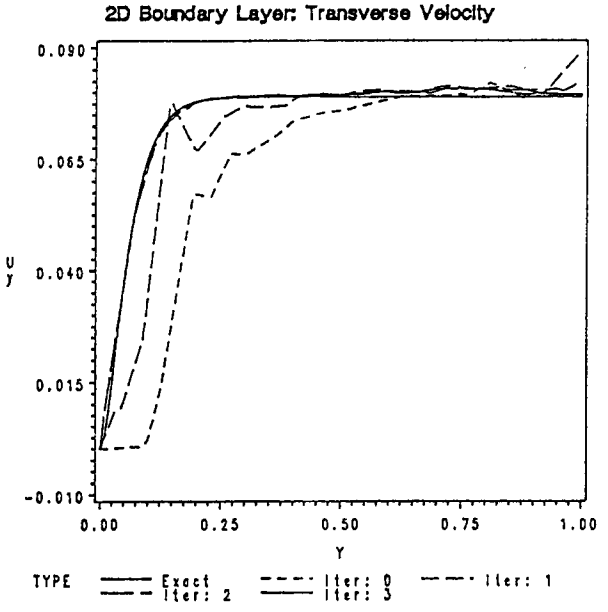

Figure 5. *2-D Boundary Layer : Convergence of v*

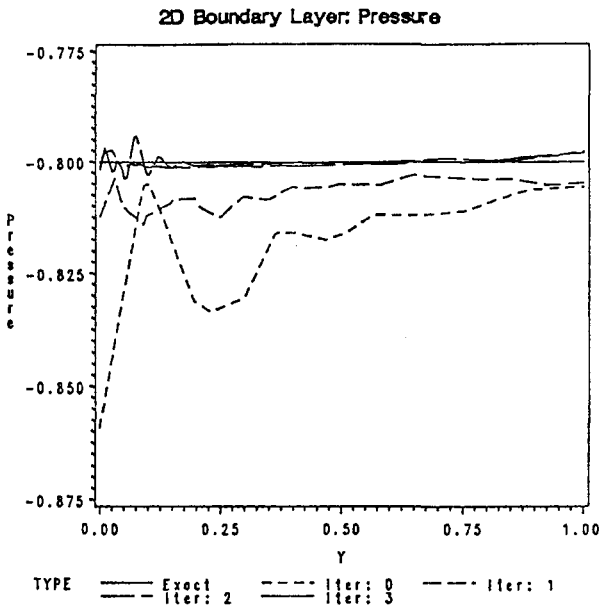

Figure 6. *2-D Boundary Layer : Convergence of p*

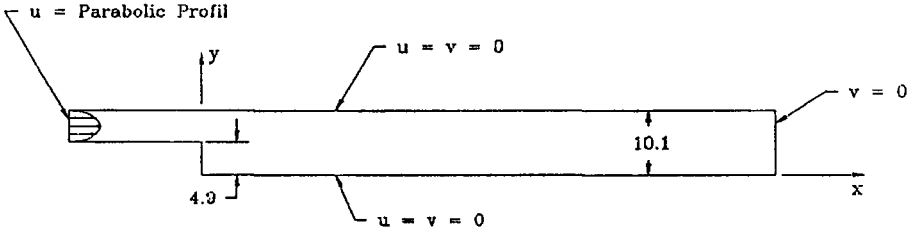

Figure 7. *Backward Facing Step*

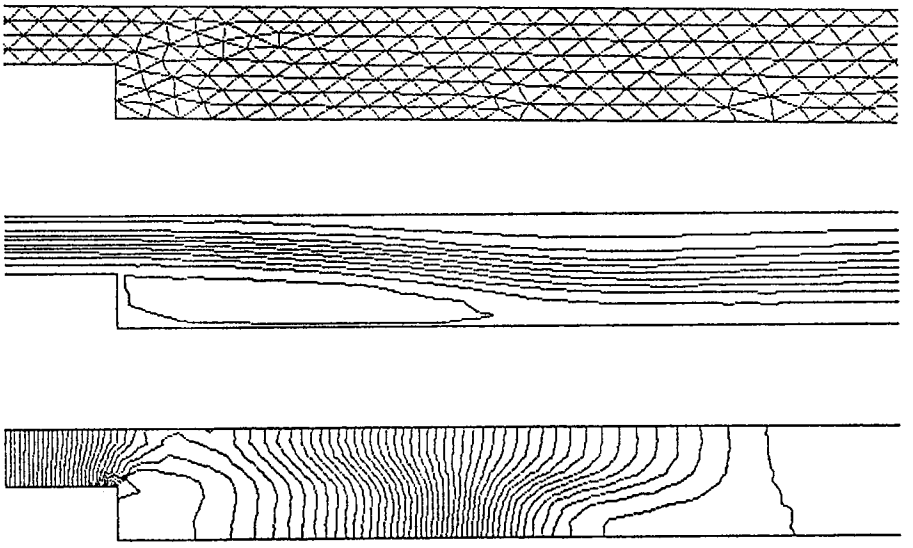

Figure 8. *Backward Facing Step : Initial mesh and solution*

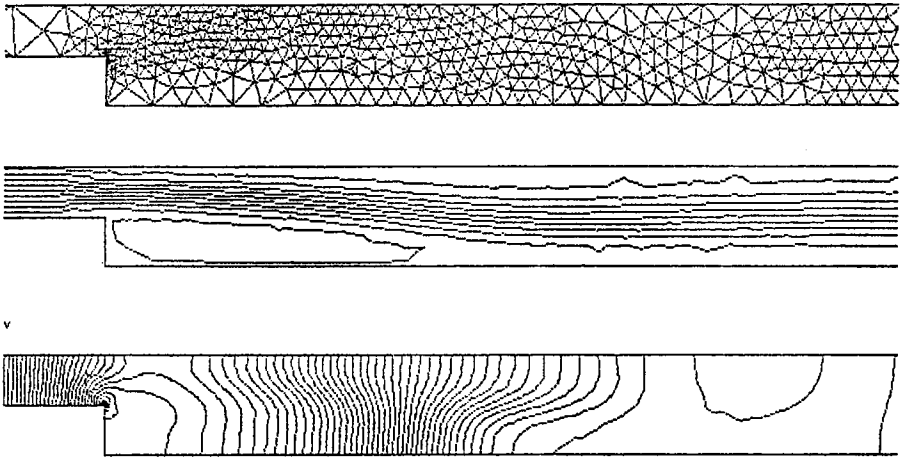

Figure 9. *Backward Facing Step : Third mesh and solution*

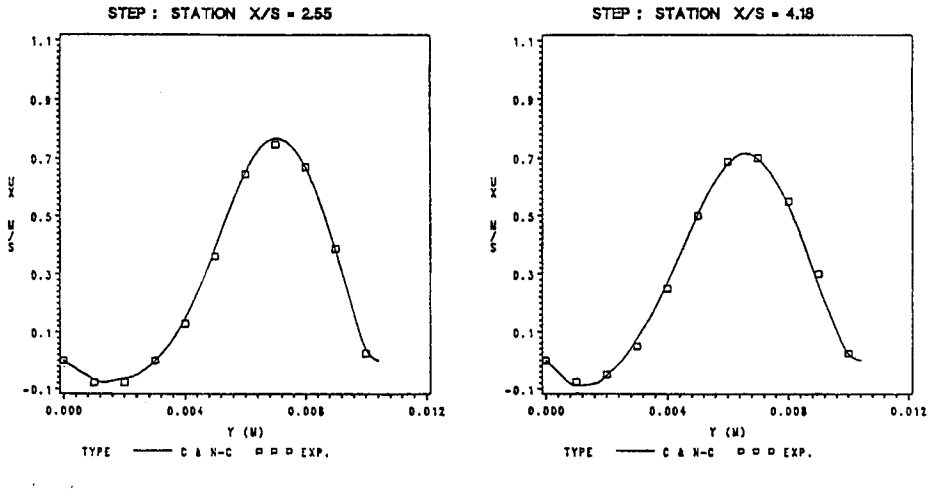

Figure 10. *Backward Facing Step : Comparison with experiments*

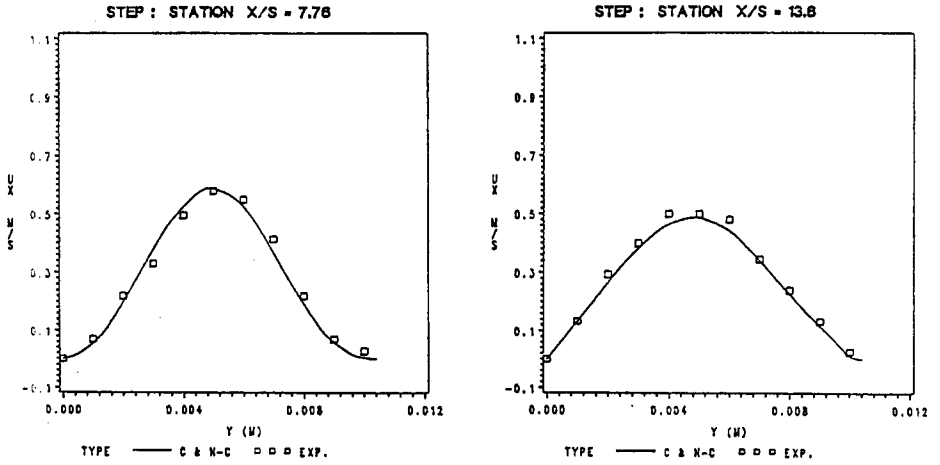

Figure 11. *Backward Facing Step : Comparison with experiments*

8 Conclusion

An error estimator for the Navier-Stokes equations has been introduced and has been shown to be reliable by solving a problem with a known analytical solution. Is was shown to be convergent in the sense that the error tends towards zero with adaptive mesh refinement.

Finally, it should be noted that the proposed error estimator is, to our knowledge, an improvement over other techniques applied on convection dominated flows. It seems to possess very stable properties even in highly non-linear situations. However, it still lacks a complete theoretical foundation to assess its limitations more thoroughly.

9 References

CRO 73 Crouzeix M. and Raviart P.A., "Conforming and con-conforming finite element methods for solving the stationary Stokes equations", RAIRO 7, rev. 3, 33–76 (1973)

FOR 83 Fortin M. and Soulié M., "A non-conforming piecewise quadratic finite element on triangles", Int. J. Numer. Meth. in Engng., Vol. 19, 505–520 (1983)

FOR 82 Fortin M., Glowinski R., "Méthodes de Lagrangien Augmentés". Dunod, Paris, 1982.

HET 90 Hétu, J.-F., Pelletier D.H., "Adaptive Remeshing for Incompressible Viscous Flows". AIAA 21th Fluid Dynamics, Plasma Dynamics and Laser Conference, June 18–20, 1990, Seattle.

ODE 86 Oden J.T., Demkowicz L., Strouboulis T., Devloo P., "Adaptive methods for problems in solid and fluid mechanics", **Accuracy estimates and adaptive refinements in finite element computations**, Edited by I. Babuska, O.C. Zienkiewicz, J. Gago, E.R. de A.Oliveira, John Wiley, New-York, 1986, 393 p.

PER 87 Peraire J., Vahdati M., Morgan K., Zienkiewicz O.C., "Adaptive Remeshing for Compressible Flows", J. Comp. Phys, Vol. 72, No 2, 1987.

PIE 93 Pierre. R., *Private communications.*

ARM 83 Armaly B.F., Durst F., Pereira J.C.F., Schong B.. "Experimental and Theoretical Investigation of Backward-facing Step Flow". J. Fluid Mech., Vol 127, pp 473–496, 1983.